Established in 1871

Swiss Medical Weekly

Formerly: Schweizerische Medizinische Wochenschrift

An open access, online journal • www.smw.ch

Original article | Published 3 October 2019 | doi:10.4414/smw.2019-20130
Cite this as: Swiss Med Wkly. 2019;149:w20130

Imaging patterns of *Pneumocystis jirovecii* pneumonia in HIV-positive and renal transplant patients – a multicentre study

Christe Andreas[a], Walti Laura[b], Charimo Jaled[a], Rauch Andri[b], Furrer Hansjakob[b], Meyer Andreas[c], Huynh-Do Uyen[c], Heverhagen Johannes T[a], Mueller Nicolas J.[d], Cavassini Matthias[e], Mombelli Matteo[e], van Delden Christian[f], Frauenfelder Thomas[g], Montet Xavier[h], Beigelman-Aubry Catherine[i], Arampatzis Spyridon[c*], Ebner Lukas[a*], Swiss Transplant Cohort Study[1] and Swiss HIV Cohort Study[2]

[a] Department of Diagnostic, Interventional and Paediatric Radiology, Inselspital, Bern University Hospital, University of Bern, Switzerland
[b] Department of Infectious Diseases, Inselspital, Bern University Hospital, University of Bern, Switzerland
[c] Department of Nephrology and Hypertension, Inselspital, Bern University Hospital, University of Bern, Switzerland
[d] Division of Infectious Diseases and Hospital Epidemiology, University Hospital Zurich, Switzerland
[e] Infectious Disease Service, Lausanne University Hospital, Lausanne, Switzerland
[f] Department of Internal Medicine, Geneva University Hospitals and University of Geneva, Switzerland
[g] Institute of Diagnostic and Interventional Radiology, University Hospital Zurich, Switzerland
[h] Division of Radiology, Geneva University Hospitals and University of Geneva, Switzerland
[i] Radiodiagnostic and Interventional Radiology, CHUV University Hospital, Lausanne, Switzerland
[1] Members of the Swiss Transplant Cohort Study: Patrizia Amico, John-David Aubert, Vanessa Banz, Guido Beldi, Christian Benden, Christoph Berger, Isabelle Binet, Pierre-Yves Bochud, Sanda Branca, Heiner Bucher, Thierry Carell, Emmanuelle Catana, Yves Chalandon, Sabina de Geest, Olivier de Rougemont, Michael Dickenmann, Michel Duchosal, Laure Elkrief, Thomas Fehr, Sylvie Ferrari-Lacraz, Christian Garzoni, Paola Gasche Soccal, Christophe Gaudet, Emiliano Giostra, Déla Golshayan, Karine Hadaya, Jörg Halter, Dimitri Hauri, Dominik Heim, Christoph Hess, Sven Hillinger, Hans H. Hirsch, Günther Hofbauer, Uyen Huynh-Do, Franz Immer, Richard Klaghofer, Michael Koller (Head of the data center), Bettina Laesser, Guido Laube, Roger Lehmann, Christian Lovis, Pietro Majno; Oriol Manuel, Hans-Peter Marti, Pierre Yves Martin, Michele Martinelli, Pascal Meylan, (Head, Biological samples management group), Nicolas J Mueller (Chairman Scientific Committee), Antonia Müller, Thomas Müller, Beat Müllhaupt, Mirjam Naegeli, Manuel Pascual (Executive office), Jakob Passweg, Klara Posfay-Barbe, Juliane Rick, Eddy Roosnek, Anne Rosselet, Silvia Rothlin, Frank Ruschitzka, Urs Schanz, Stefan Schaub, Aurelia Schnyder, Christian Seiler, Jan Sprachta; Susanne Stampf, Jürg Steiger (Head, Executive Office), Guido Stirnimann, Christian Toso, Christian Van Delden (Executive office), Jean-Pierre Venetz, Jean Villard, Madeleine Wick (STCS coordinator), Markus Wilhelm, Patrick Yerly.
[2] Members of the Swiss HIV Cohort Study: Aebi-Popp K, Anagnostopoulos A, Battegay M, Bernasconi E, Böni J, Braun DL, Bucher HC, Calmy A, Cavassini M, Ciuffi A, Dollenmaier G, Egger M, Elzi L, Fehr J, Fellay J, Furrer H, Fux CA, Günthard HF (President of the SHCS), Haerry D (deputy of "Positive Council"), Hasse B, Hirsch HH, Hoffmann M, Hösli I, Huber M, Kahlert CR (Chairman of the Mother & Child Substudy), Kaiser L, Keiser O, Klimkait T, Kouyos RD, Kovari H, Ledergerber B, Martinetti G, Martinez de Tejada B, Marzolini C, Metzner KJ, Müller N, Nicca D, Paioni P, Pantaleo G, Perreau M, Rauch A (Chairman of the Scientific Board), Rudin C, Scherrer AU (Head of Data Centre), Schmid P, Speck R, Stöckle M (Chairman of the Clinical and Laboratory Committee), Tarr P, Trkola A, Vernazza P, Wandeler G, Weber R, Yerly S.

* Contributed equally to the work

Author contributions
Guarantors of integrity of entire study: LE, SA, AC. Study concepts/study design or data acquisition or data analysis/interpretation: all authors. Manuscript drafting or manuscript revision for important intellectual content: all authors. Approval of final version of submitted manuscript: all authors. Literature research: LE, SA, AC. Statistical analysis: AC. Manuscript editing: all authors

Correspondence:
Prof. Lukas Ebner, MD, Department of Diagnostic Radiology, Freiburgstreet 10, CH-3010 Bern, lukas.ebner[at]insel.ch

Summary

OBJECTIVES: To investigate differences in chest computed tomography (CT) and chest radiographs (CXRs) of *Pneumocystis jirovecii* pneumonia (PJP) between renal transplant recipients (RTRs) and human immunodeficiency virus (HIV)-positive patients.

METHODS: From 2005 to 2012, 84 patients with PJP (RTR n = 24; HIV n = 60) were included in this retrospective multicentre study. Written informed consent was obtained. CT scans and CXRs were recorded within 2 weeks after the onset of symptoms. PJP diagnosis was confirmed either by cytology/histology or successful empirical treatment. Two blinded radiologists analysed the conventional chest films and CT images, and recorded the radiological lung parenchyma patterns, lymph node enlargement and pleural pathologies (pneumothorax, effusion). The radiological features of the two subgroups were compared.

RESULTS: Consolidations and solid nodules prevailed on CT in RTRs (91.7 ± 5.6% vs 58.3 ± 6.4% with HIV, p = 0.019 and 91.7 ± 5.6% vs 51.6 ± 6.5% with HIV, p = 0.005). HIV-positive patients with PJP showed more atelectasis (41.7 ± 6.4% vs 4.2 ± 4.1% in RTRs, p = 0.017) and hilar lymph node enlargement (23.3 ± 5.5% vs 0.0 ± 0.0% in RTRs, p = 0.088). Ground glass opacification was found in all cases. Pneumothorax was a rare complication, occurring in 3% of the HIV-positive patients; no pneumothorax was found in the RTRs. On CXR, the basal lungs were more affected in HIV-positive patients as compared with RTRs (p = 0.024).

CONCLUSIONS: PJP on CT differs substantially between RTRs and HIV-positive patients. Physicians should be aware of such differences in order not to delay treatment, particularly in renal transplant recipients.

***Keywords**: lung, pneumocystis pneumonia, kidney transplantation, HIV, multislice computed tomography*

Introduction

Based on recent studies, diseases of the respiratory tract still represent a leading cause of morbidity and mortality in immunocompromised individuals. In particular, pneumonia is a feared complication in solid organ recipients and human immunodeficiency virus (HIV)-positive patients. These groups of immunocompromised patients are particularly afflicted by atypical pneumonias due to viral and fungal pathogens, including *Pneumocystis jirovecii* pneumonia (PJP) [1, 2].

PJP may present with a very variable pattern of clinical and radiological manifestations, depending on the immunological status of the patient. Whereas in HIV-positive individuals the clinical manifestations of PJP are rather subacute with slow progression, transplanted patients under continued immunosuppression experience a more aggressive disease with poor survival rates [3, 4]. Similar to the varying clinical manifestations, the radiological imaging features of PJP may exhibit a very broad spectrum of patterns with predominantly ground glass opacities, septal thickening, subpleural sparing and cysts [5–7]. A recently published study showed that the current clinical course of PJP in immunocompromised patients is rather subtle and rarely life threatening. In addition, these results suggested that, compared with renal transplant recipients (RTRs), enlarged hilar lymph nodes, areas of diffuse infection and ground glass nodules were a specific radiological imaging feature of PJP in HIV-positive patients.

The primary aim of the current multicentre, multi-cohort study was to further explore the computed tomography (CT) and chest X-ray imaging features of PJP in a sufficient number of immunocompromised patients from two well-defined cohorts, the Swiss HIV Cohort Study (SHCS) [8] and RTRs included in the Swiss Transplant Cohort Study (STCS) [9]. We hypothesised that the imaging patterns on CT differ substantially between HIV patients and RTRSs.

Material and methods

This multicentre, multi-cohort study was conducted as a retrospective cross-sectional registry analysis of confirmed PJP cases retrieved from the SHCS and the STCS. Written informed consent was obtained according to both cohorts' registry regulations. Ethical approval from the SHCS and written informed consent from all participants was obtained. For the RTRs ethical approval from the cantonal ethic committee of Bern was granted for the retrospective analysis. From 2005 to 2012, databases of the two national cohorts were screened for PJP cases. Our cohort includes data from four university hospitals. The diagnosis of PJP was established by cytology and/or histology, as well as clinical responsiveness and radiological resolution under PJP treatment (trimethoprim/sulfamethoxazole). Concomitant cytomegalovirus infection was excluded by polymerase chain reaction analysis in all patients. According to the national study registries for HIV patients and solid organ transplant recipients, a definitive diagnosis was established by cytology/microscopy or histology. However, a presumptive diagnosis of PJP is possible under the following conditions:

If on PJP prophylaxis: history of dyspnoea on exertion, or non-productive cough (within 3 months); typical appearance of diffuse bilateral pulmonary infiltrate, and no bronchoscopy done or negative bronchoscopy after having received at least 1 week of PJP treatment; no evidence of bacterial pneumonia, and response to PJP treatment.

If not on PJP prophylaxis for at least 2 weeks and CD4 count less than 200: history of dyspnoea on exertion, or non-productive cough (within 3 months); chest radiograph normal, atypical or typical for PJP, and no bronchoscopy done or negative bronchoscopy after having received at least 1 week of PJP treatment; no evidence of bacterial pneumonia, and response to PJP treatment.

Additionally, we collected all conventional chest radiographs available within a 2-week period after the onset of symptoms. After the identification of suitable patients, the clinical and imaging data at the tertiary care centre were anonymised and transferred to our institution for further analysis.

Image acquisition

The CT scans were made on different generations of scanner from various vendors. The scanners comprised 4-, 16-, 64- and 128-row scanners (Siemens, Germany; Philips, Netherlands, General Electric, USA) applying a slice thickness of 1 to 2 mm. The scan range was constant, starting at the thoracic inlet and caudally including the whole lung and adrenal glands. Automated tube current modulation using reference milliampere seconds (mAs) was implemented on the scanners whenever applicable. Additionally, care kilo voltage (kV) was used whenever available. Chest radiographs were acquired in a prone position and in two planes (posterior-anterior view and lateral view).

Image interpretation

The read out and pattern annotation was performed by two subspecialised radiologists in consensus with 6 and 15 years, respectively, of expertise in the field. The radiologists were informed that the study population consisted of patients with confirmed pneumocystis pneumonia; however, the readers were unaware of the underlying condition (HIV versus renal transplantation).

Prior to the read out, the cases were randomised. The reading was carried out on a standard picture achieving and communication system (PACS Sectra, Linköping, Sweden). All CT scans were reviewed in a standardised lung stetting with a window level of −600 Hounsfield units (HU) and a window width of 1600 HU, reconstructed with a dedicated lung kernel (B/I 70f). For the evaluation of the soft tissues (the mediastinum), we used a soft tissue kernel reconstruction (B/I 30) in combination with a window level of 50 HU and a window width of 450 HU. In a separate reading session, the chest radiographs were analysed. The readers were unaware of the patients' underlying disease as well as the chest CT findings, and the images were

ABBREVIATIONS:

CT	computed tomography
HIV	human immunodeficiency virus
PJP	*Pneumocystis jirovecii* pneumonia
RTR	renal transplant recipient

randomised prior to the read out. The patterns were classified according to the Fleischner Society glossary of terms [10]. The following patterns were evaluated by the readers: consolidation (defined as increased lung density without contrast enhancement representing infiltration), reticulation, ground glass (diffuse, patchy, mosaic pattern), nodules (solid, subsolid), cysts, signs of fibrosis (honeycombing), airways (cuffing, mucus plugging, bronchiectasis), and pleural alterations (thickening, effusion). Furthermore, the readers evaluated the lymph nodes in the mediastinum and in the hilar regions. The mediastinal and hilar lymph nodes were assessed in a soft tissue window; lymph node enlargement was defined as a short axis diameter ≥1cm. In total, both radiologists recorded 43 radiographic findings. The distribution of parenchymal changes within the lung was recorded according to the segmental anatomy of the lungs (10 segments on the left and 10 segments on the right). Additionally, we further assessed the disease location within the right and left lung: central-perihilar changes versus peripheral-subpleural changes as well as diffuse affection of the lungs. Parenchymal changes showing a subpleural sparing were recorded separately.

The classification of imaging patterns is described in more detail in appendix 1.

Statistics

Continuous data were compared using Student's t test if normally distributed; otherwise, the Mann-Whitney test was applied. Statistical analyses of non-continuous dichotomous data were compared using the chi-square test or Fisher's exact test. The absolute frequency of each lung pattern was recorded and compared between groups. The standard error of frequency was assessed. All p-values were two-sided, and the level of significance was set to 0.05. A *post hoc* Bonferroni test was applied to evaluate significant differences between each assessed value. The five most frequent groups of patterns were corrected by a factor of five; all other pattern and location variables were corrected according to the number of variables. Additionally, a multiple logistic regression model was applied. The statistical analysis was performed with MedCalc Version 7.6.0.0 statistical software (MedCalc Software, Ostend, Belgium).

Results

After applying the inclusion criteria, a total of 84 patients with confirmed PJP were included in this study population. We identified 24 renal transplant recipients (30%) and 60 HIV patients (70%) with PJP (demographic data are summarised in table 1).

Computed tomography findings

A total of 47 different chest patterns were recorded in the reading sessions, including pleural alterations and lymph node enlargement. As compared with HIV, consolidations and solid nodules (fig. 1) were more frequent in RTRs (91.7 ± 5.6% vs 58.3 ± 6.4% with HIV, p = 0.019 and 91.7 ± 5.6% vs 51.6 ± 6.5% with HIV, p = 0.005, respectively; table 2). All RTRs had ground glass opacifications, whereas none had enlarged hilar lymph nodes.

In comparison, the HIV-positive patients with PJP showed significantly more areas of atelectasis (41.7 ± 6.4%, vs 4.2 ± 4.1% in RTRs, p = 0.017; table 2). Furthermore, HIV patients tended to present with a more "classic" pattern of PJP, exhibiting subpleural sparing (fig. 2) and additional hilar lymph node enlargement (23.3 ± 5.5%; fig. 3). Pneumothorax formation was restricted to 3.3% of the HIV-positive patients. When the results from the conservative Bonferroni method were compared with the results from a multi-variable analysis, significantly more cysts could be found in HIV than in RTR cases (15.0 ± 4.6% vs 4.2 ± 4.1%, p = 0.038; table 2). An analysis of the disease distribution within each lung segment between the two cohorts did not yield any statistically significant results (table 2).

Chest radiograph findings

The patterns for each chest radiograph were recorded (table 3). Overall, there were no differences in patterns between the two cohorts according to the Bonferroni corrected results. However, the results from the logistic regression model showed that there was a significantly higher preva-

Table 1: Demographic information.

		RTR group		HIV group	
Total N		24		60	
Gender (M:F)		15:9		42:18	
Median age (years, range)		64	39–70	43	25–76
Median time from transplantation / HIV diagnosis to PJP (days, years, range)		2y	(0–11y)	45d	(0d–27y)
CD4 count (cl/ml), median (IQR)		n/a		79	(3–436)
Underlying disease in RTRs	ADPKD	7	29.2%	–	
	IgA-nephropathy	5	20.8%	–	
	Diabetic nephropathy	6	25.0%	–	
	Chronic tubular interstitial nephropathy	3	12.5%	–	
	Focal segmental glomerulosclerosis	2	8.3%	–	
	Mesangioproliferative glomerulonephritis	1	4.2%	–	
HIV risk group	Injection drug user	–		7	11.7%
	Men who have sex with men	–		21	35.0%
	High risk heterosexuals	–		28	46.7%
	Unknown	–		4	6.7%
	HIV diagnosis made following PJP	–		13	21.7%

ADPKD = autosomal dominant polycystic kidney disease; HIV = human immunodeficiency virus; n/a = not applicable; PJP = *Pneumocystis jirovecii* pneumonia; RTR = renal transplant recipient

lence of reticulation in RTRs as compared with HIV patients (95.7 ± 4.2% vs 86.0 ± 4.5%; table 3). Consolidations and solid nodules were found in 47.8 ± 10.2% and 4.3 ± 4.2% of RTRs, respectively. Consolidation and multiple nodules were more prevalent in the HIV-positive patient cohort (fig. 4). For the pattern distribution within the lung lobes, we found that the basal lungs, namely, middle lobe, lingula and lower lobes, were significantly more affected in HIV-positive patients (75.0 ± 5.6% vs 58.7 ± 10.1% in RTRs p = 0.021; fig. 5). In particular, the middle lobe was mainly involved in the HIV-positive cohort (64.0 ± 6.2% vs 17.4 ± 7.7% in RTRs, p = 0.006; table 3).

Discussion

The aim of the present study was to investigate the PJP-related imaging patterns on CT and chest radiography in

Figure 1: Axial computed tomography (CT) image from a renal transplant recipient. Typical CT image findings of a renal transplant recipient: patchy consolidations are found in the right upper lobe as well as in the apical segment of the left lower lobe (asterisk). There is also diffuse ground glass opacification present (blue arrow); of note, slight subpleural sparing can be seen in the anterior upper lobes. Solid nodules (red arrows) are also present in the periphery of the right upper and lower lobe.

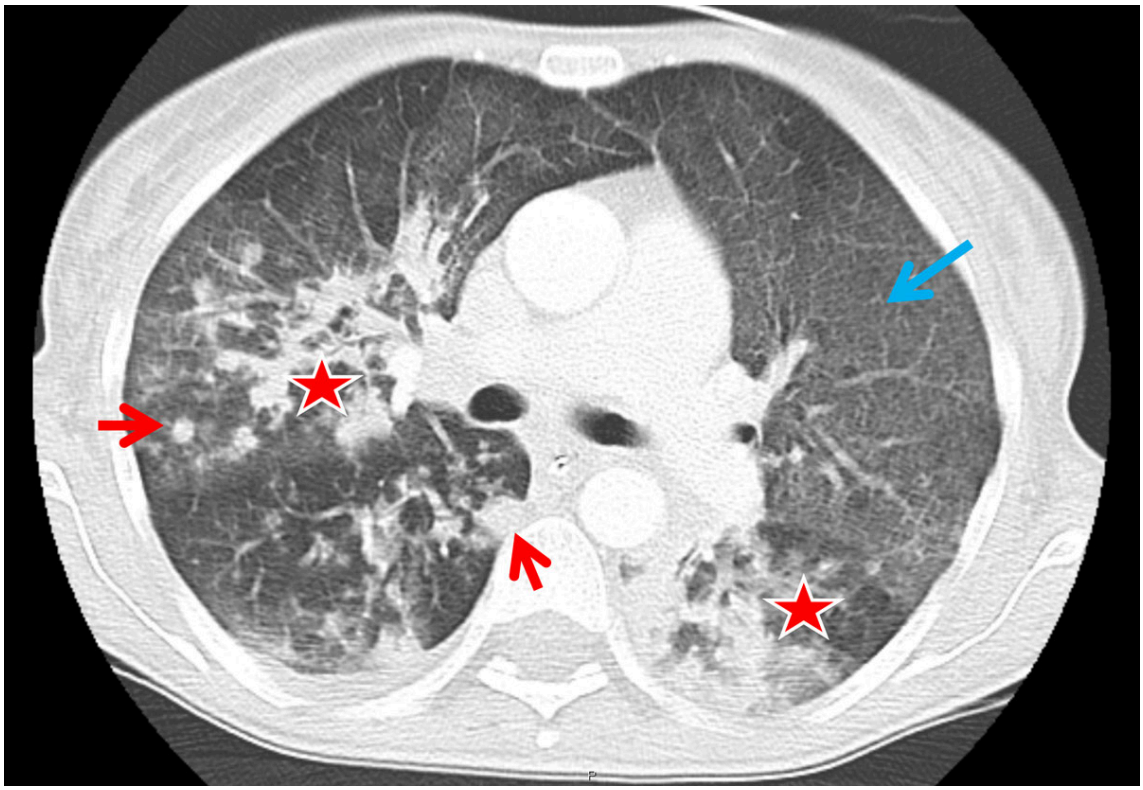

Table 2: *Pneumocystis jirovecii* pneumonia lung patterns and locations on computed tomography.

Pattern		RTR (% ± SD)	HIV+ (% ± SD)	p-value	p-value*
Consolidation		91.7 ± 5.6	58.3 ± 6.4	**0.018**	**0.002**
Atelectasis		4.2 ± 4.1	41.7 ± 6.4	**0.017**	**0.016**
Reticulations		83.3 ± 7.6	66.7 ± 6.1	0.91	0.383
Ground glass	Diffuse	66.7 ± 9.6	58.3 ± 6.4	1.00	0.604
	Patchy	87.5 ± 6.8	66.7 ± 6.1	0.68	0.062
	Mosaic	37.5 ± 9.9	28.3 ± 5.8	1.00	0.413
Ground glass nodules	Any	100 ± 0.0	96.7 ± 2.3	1.00	0.432
	GGN	75.0 ± 8.8	68.3 ± 6.0	1.00	0.799
	Solid	91.6 ± 5.6	51.6 ± 6.5	**0.005**	**0.004**
	Mixed	12.5 ± 6.8	23.3 ± 5.5	1.00	0.068
Nodules	Any	95.8 ± 4.1	76.7 ± 5.5	**0.009**	**0.040**
Cysts		4.2 ± 4.1	15.0 ± 4.6	1.00	**0.038**
Hilar lymph nodes		0.0 ± 0.0	23.3 ± 5.5	0.088	0.984
Mediastinal lymph nodes		33.3 ± 9.6	43.3 ± 6.4	0.466	0.238
Location	Central	75 ± 8.8	55 ± 6.4	0.42	0.113
	Peripheral	91.7 ± 5.6	75 ± 5.6	0.4	0.689
	Multifocal	79.2 ± 8.3	50 ± 6.4	**0.047**	**0.249**
	Diffuse	66.7 ± 9.6	70 ± 5.9	1.00	0.581
	Subpleural sparing	16.7 ± 7.6	51.7 ± 6.5	**0.01**	**0.020**

GGN = ground glass nodules; SD = standard deviation Significant results are displayed in bold font * p-values from logistic regression

HIV-positive and renal transplant patients. Our results indicate that there are distinct radiological patterns on CT scans, but not on radiographs, within both groups.

The PJP radiological CT findings in renal transplant patients were dominated by multifocal consolidation and solid nodularities, whereas in the HIV population more classic subpleural sparing was present. A common feature in both groups was ground glass opacification, a finding also previously reported by Tasaka et al. [11] when comparing PJP features in oncological patients and HIV patients. Hardak et al. [5] also reported extensive ground glass densities in a mixed patient population with PJP. Ground glass opacification therefore has a high sensitivity for PJP and a lack of this feature seems to rule out PJP with a high level of certainty, irrespective of aetiology of underlying immunosuppression. The finding of atelectasis is reported to be infrequent in patients with PJP. However, in the data presented here, atelectasis was a significant finding in patients with HIV. It has been reported previously that patients with HIV and PJP have a larger pneumocystis burden and reduced neutrophil count when compared with PJP patients without HIV. Although not evaluated in this study, this might be a factor in the development of atelectasis in these patients. Another contributing factor might be the presence of excessive foam-like exudate in the alveoli, which is a considered a typical finding in microscopy. The foamy exudate in combination with hyaline membrane formation and granulomatous inflammation, also microscopic findings in PJP, might explain the higher prevalence of atelectasis in the HIV cohort.

Prevalence of subpleural sparing has frequently been reported in HIV-related PJP cases [12, 13]. This finding was also evident in the presented data; however, it mainly applied to HIV patients. In RTRs, subpleural sparing was found in only a minority of patients. Furthermore, micronodules showed a high prevalence in the transplant population, whereas they were exceedingly rare in the HIV group. Another important finding in this study population was that hilar lymph node enlargement was exclusively found in HIV-positive individuals. Previous studies, however, showed that PJP is rarely associated with lymphadenopathy on imaging studies [14]. These diverging imaging manifestations may reflect the effect of the different aetiology of immunosuppression on the radiological appearance of PJP [15].

Of note, pulmonary cysts, previously described as a hallmark feature in PJP, were present in only 4% of the HIV-positive patients and in none of the RTRs. With the advance of prophylaxis in high-risk groups, this classic complication is now an infrequent finding.

Besides the previously described diffuse lung effects in HIV patients [10], this multicentre cohort demonstrated also patterns that were multifocally distributed. Additionally, the predominance of ground glass nodules in the RTR patients could not be confirmed; instead, we found more solid nodules. Whereas in a previous study, HIV patients and transplant recipients exhibited subpleural sparing, the

Figure 2: Computed tomography (CT) findings in a human immunodeficiency virus-positive patient suffering from *Pneumocystis jirovecii* pneumonia (PJP) (axial CT section at the level of the lung bases): diffuse ground glass opacity (asterisk) and subpleural sparing (arrows) was found to represent a more or less classic CT-pattern for PJP.

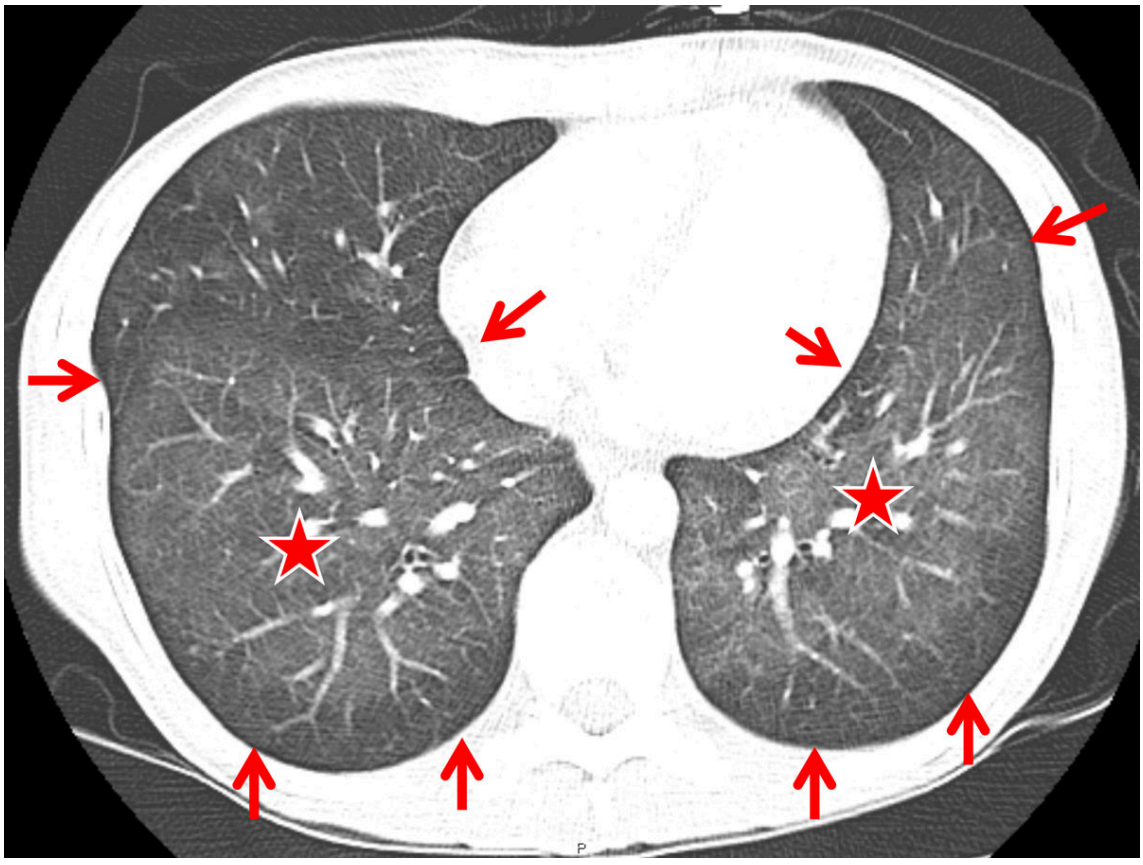

recent analysis revealed that this feature was foremost in HIV-associated cases of PJP [7]. In contrast, both studies found no enlarged lymph nodes in renal transplant patients.

Differences in the presentation of PJP between HIV and RTR cases could reflect immunological differences between HIV- and transplant-associated immunodeficiencies. For example, the immune system is ceasing in HIV-positive patients, but is suddenly and continuously suppressed by therapy in RTR. However, this remains speculative and we will explore this finding in further studies primarily focusing on the manifestation pathway.

The most common clinical signs were subtle in both groups and the duration from illness onset to hospital presentation was longer in the HIV patients, implying a less fulminant clinical course. The higher prevalence of atelectasis in HIV patients might reflect the more chronic nature of PJP in this population. On the other hand, most RTR PJP cases occurred several months (>12 months) after successful transplantation, with no prophylactic treatment at PCP diagnosis and with a suspected viral upper respiratory tract infection. Thus, the significant presence of consolidation in RTRs might reflect a concurrent infection with oth-

Figure 3: Axial cross section image in soft tissue window at the level of the carina in a human immunodeficiency virus (HIV)-positive patient with *Pneumocystis jirovecii* pneumonia (PJP). There is mediastinal lymph node enlargement at the left and right lower paratracheal nodal stations (arrows). Although not specific for PJP in HIV-positive individuals, mediastinal lymph node enlargement was more frequent in this patient population. TR = trachea; SVC = superior vena cava; PA = pulmonary artery; AO = aorta

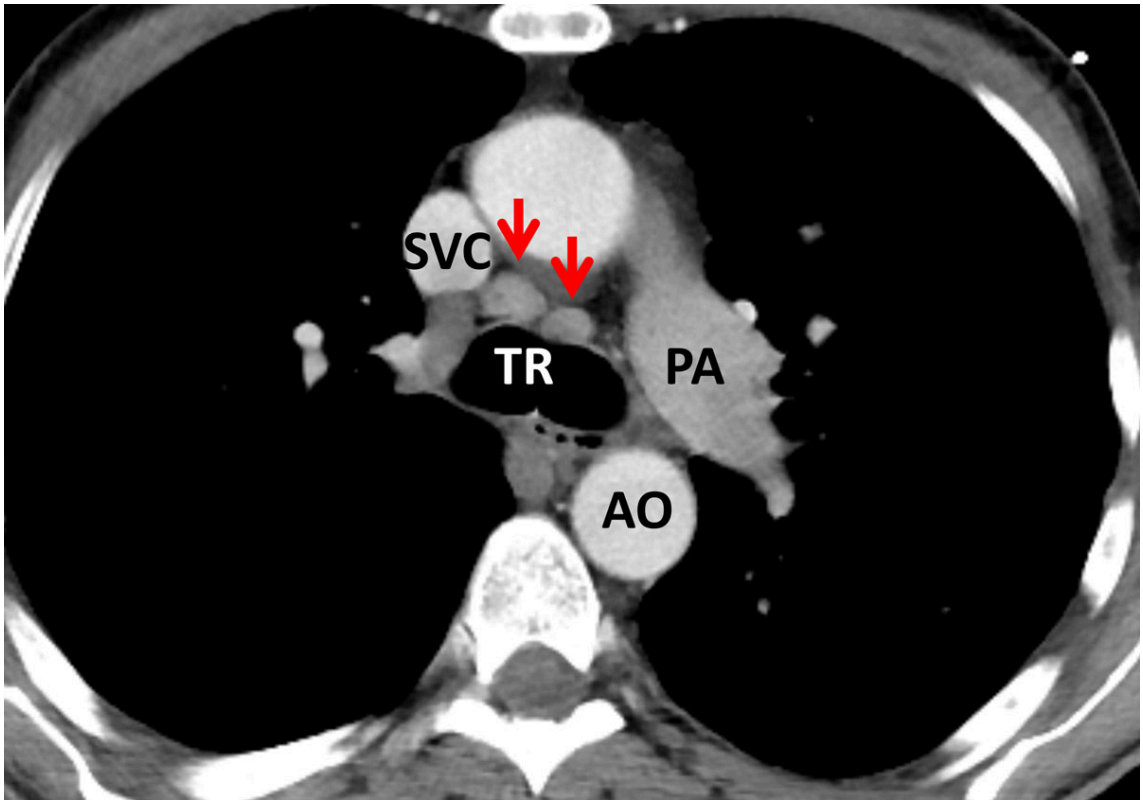

Table 3: *Pneumocystis jirovecii* pneumonia patterns on chest radiographs.

Pattern		RTR (% ± SD)	HIV+ (% ± SD)	p-value*	p-value†
Opacity	Acinar	47.8 ± 10.2	54.0 ± 6.4	1	0.587
	Reticulation	95.7 ± 4.2	86.0 ± 4.5	1	**0.034**
Nodules	Solitary	4.3 ± 4.2	2.0 ± 1.8	1	0.820
	Multiple	4.3 ± 4.2	12.0 ± 4.2	1	0.247
PJP-specific	Cysts	0.0 ± 0.0	8.0 ± 3.5	1	0.983
	Subpleural sparing	0.0 ± 0.0	2.0 ± 1.8	1	0.992
	Pneumothorax	0.0 ± 0.0	4.0 ± 2.5	1	0.988
Distribution	Right upper lobe	56.5 ± 10.1	72.0 ± 5.8	1	0.335
	Middle lobe	17.4 ± 7.7	64.0 ± 6.2	1	**0.006**
	Right lower lobe	91.3 ± 5.8	86.0 ± 4.5	1	0.113
	Left upper lobe	69.6 ± 9.4	72.0 ± 5.8	1	0.560
	Lingula	34.8 ± 9.7	62.0 ± 6.3	1	0.735
	Left lower lobe	91.3 ± 5.8	88.0 ± 4.2	1	0.629
	Lower lung‡	58.7 ± 10.1	75.0 ± 5.6	**0.021**	n/a
Symmetry		69.8 ± 19.0	74.9 ± 26.0	0.86	n/a

HIV = human immunodeficiency virus; PJP = *Pneumocystis jirovecii* pneumonia; RTR = renal transplant recipient; SD = standard deviation * Bonferroni corrected p-values (factor 15) † p-values from logistic regression ‡ lower lobe + middle lobe / lingula

er pathogens. In addition, the higher prevalence of small nodules in RTRs, in combination with ground glass opacifications, most likely represent ongoing or chronic alveolitis.

We found that cystic lung changes were significantly more frequent in HIV patients. This phenomenon has been encountered previously. In fact, the prevalence of cysts in PJP has declined, presumably owing to prophylactic therapy in high-risk populations. However, there is still a discrepancy between RTR and HIV patients, with the latter showing more cystic changes. One explanation could be that a considerable number of these patients show less compliance with treatment or slower disease progression than the transplant patients. Another reason might be the clinical presentation.

Finally, when we look at the time of symptom onset, we struggle to provide specific data. This is also a clinical problem, since the symptom onset in RTRs is acute, whereas in HIV patients we observed a more indolent course of symptoms. Based on the different clinical presentation, it is possible that some of the imaging differences may reflect different time points of investigation. Presumably, RTRs show the acute manifestation of PJP and imaging features of PJP in HIV patients represent a subacute to chronic spectrum of the disease. In this study, several significant differences in CT findings between HIV-associated PJP and renal transplant-associated PJP were found; however, only a few differences could be defined on chest radiographs. This reflects the limited capabilities of chest radiography for the disease characterisation, in particular in cases of atypical pneumonia.

Analysing the demographic data of both cohorts, we found a substantial difference in the median time from renal transplantation and HIV diagnosis to PJP. In the RTR group, the disease occurred several years after transplantation, when patients were without any chemoprophylaxis for PJP; in the HIV group, this was only 45 days. However, both groups showed a substantial time range (0–11 years in RTRs vs 0–27 years in HIV patients). This might explain the differences in imaging features. In addition, the possibility of PJP breakthrough in the RTR cohort may have played a role in the similar clinical and radiological manifestation of the disease.

Our study has some limitations. The sample size is relatively small, especially for a multicentre study design. Statistically, this issue has been addressed by using a conservative Bonferroni correction to balance the different cohort sizes. Furthermore, both cohorts use different definitions of PJP infection, which could have affected the interpretation. Also, the study population also contained subjects with non-contrast CT scans, mainly because of limited renal function especially in RTRs. The detection of hilar lymph nodes on non-contrast CT scans can be challenging and particular focus should centre on the lymph node as-

Figure 4: Bilateral nodular consolidation in a human immunodeficiency virus -positive patient.

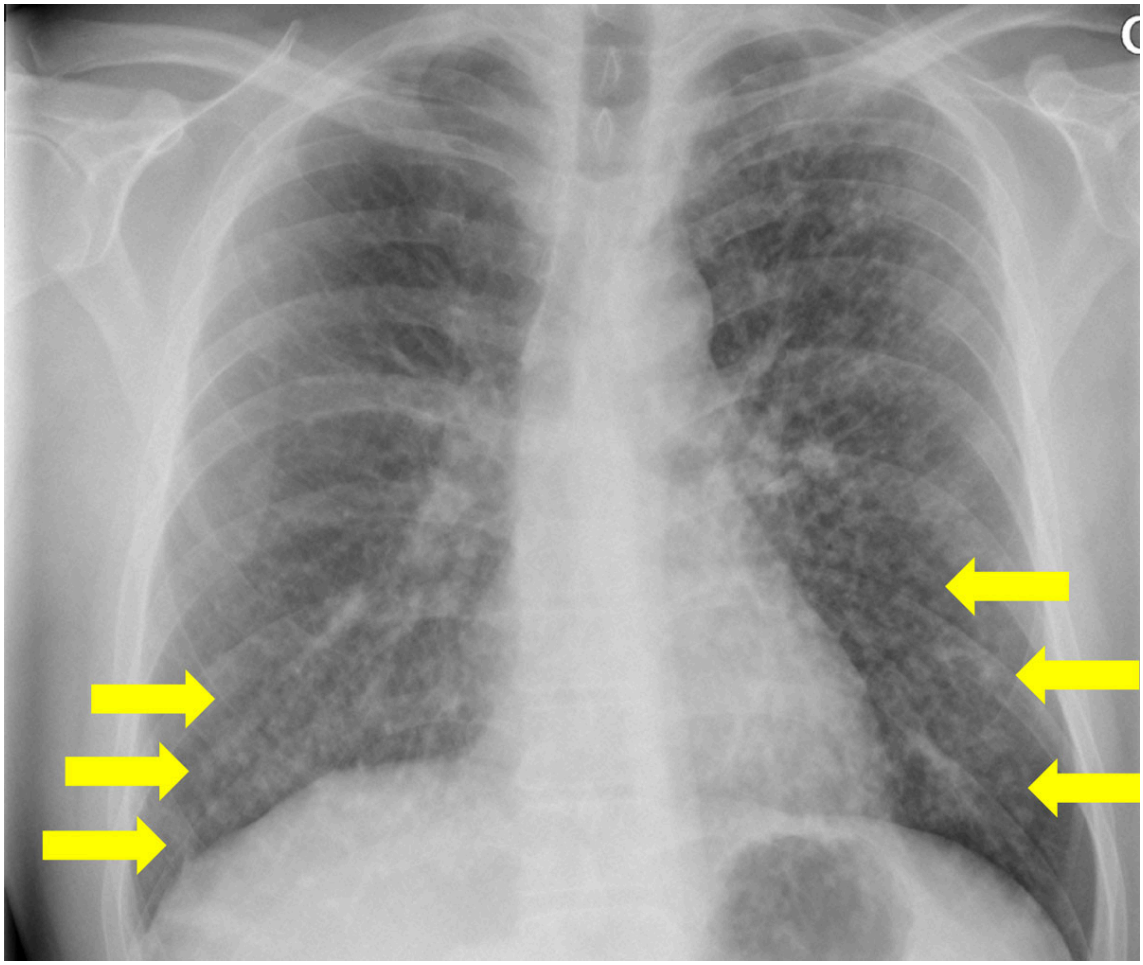

Figure 5: Faint homogeneous central ground glass opacity with sparing of the caudal lungs/sinus phrenicocostalis (arrows) in a renal transplant patient.

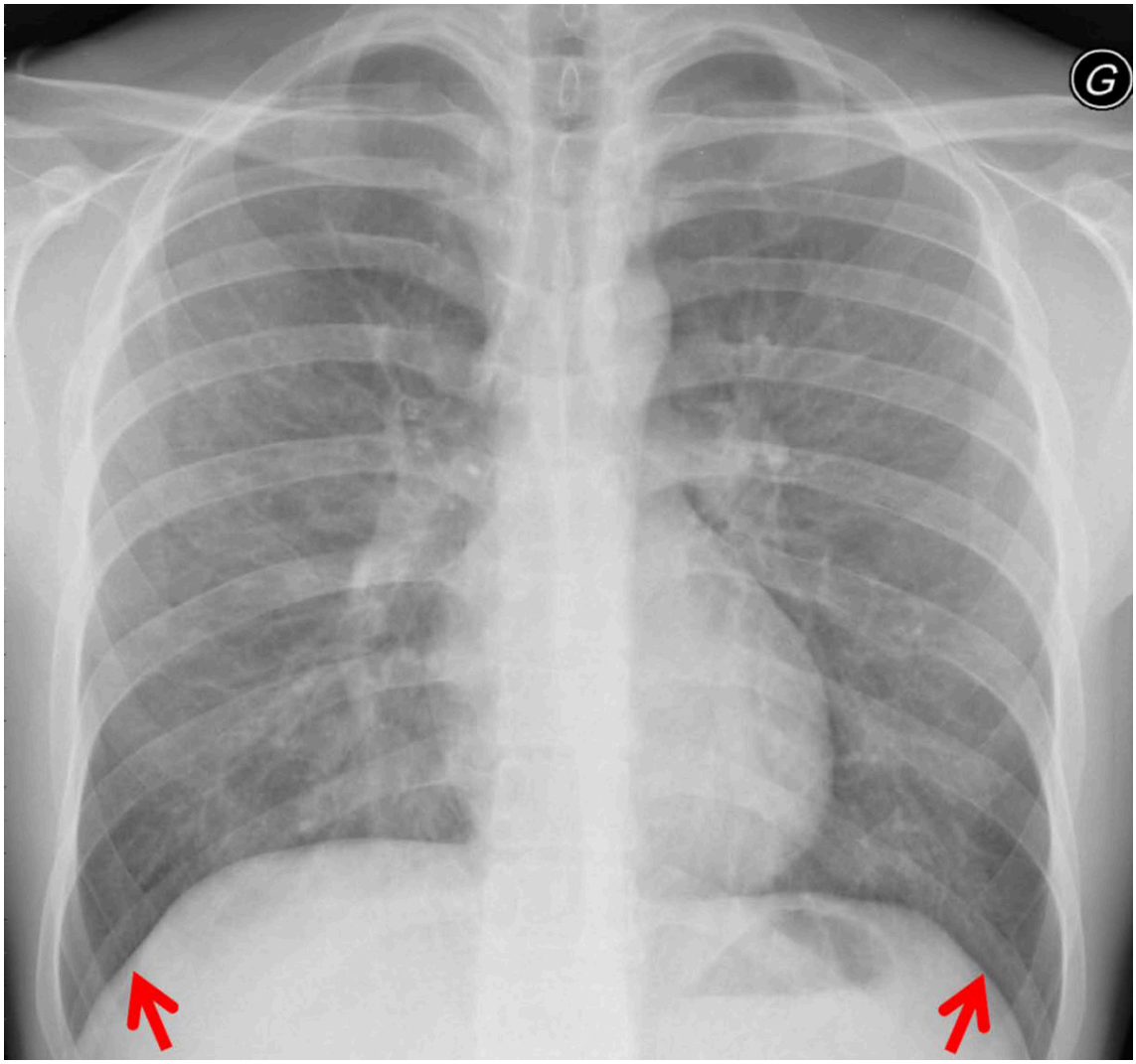

sessment in those cases. Finally, the period between imaging and disease onset of 2 weeks is relatively long and might have impaired the study results.

In summary, the extension of our study to the national level based on confirmed PJP cases coming from four tertiary hospitals revealed a rather variable but disease-specific manifestation pattern of PJP, most likely attributable to the underlying aetiology of immunosuppression. Indeed, whereas CD4 cell counts below 200 cell/ml are a clearly identified risk factor for PJP in the HIV-positive population, such an association has not been established in the transplant population so far, supporting the hypothesis that the distinct underlying conditions led to different types of immunosuppression. Based on the differing imaging manifestations of PJP in transplant recipients and HIV-positive patients, it is of utmost importance for radiologists to be aware of the spectrum of patterns in the context of different underlying diseases and to show high awareness in high-risk groups.

Data availability

This study was conducted in the framework of the Swiss Transplant Cohort Study and the Swiss HIV Cohort Study supported by the Swiss National Science Foundation and the Swiss University Hospitals (G15) and transplant centres. Requests for data access must be submitted to the STCS and/or SHCS and are subject to review by the Scientific Committees (www.stcs.ch/about/study-description; www.shcs.ch/).

Financial disclosure

This study was financed within the framework of the Swiss HIV Cohort Study, supported by the Swiss National Science Foundation (grant no. 177499), by Swiss HIV Cohort Study SHCS project no. 756, by Swiss Transplant Cohort Study STCS, project no. 055, and by the SHCS research foundation.

Potential competing interests

The authors declare no competing interests.

References

1 Franquet T, Giménez A, Hidalgo A. Imaging of opportunistic fungal infections in immunocompromised patient. Eur J Radiol. 2004;51(2):130–8. doi: http://dx.doi.org/10.1016/j.ejrad.2004.03.007. PubMed.

2 Castañer E, Gallardo X, Mata JM, Esteba L. Radiologic approach to the diagnosis of infectious pulmonary diseases in patients infected with the human immunodeficiency virus. Eur J Radiol. 2004;51(2):114–29. doi: http://dx.doi.org/10.1016/j.ejrad.2004.03.008. PubMed.

3 Goto N, Oka S. Pneumocystis jirovecii pneumonia in kidney transplantation. Transpl Infect Dis. 2011;13(6):551–8. doi: http://dx.doi.org/10.1111/j.1399-3062.2011.00691.x. PubMed.

4 Fritzsche C, Riebold D, Fuehrer A, Mitzner A, Klammt S, Mueller-Hilke B, et al. Pneumocystis jirovecii colonization among renal transplant recipients. Nephrology (Carlton). 2013;18(5):382–7. doi: http://dx.doi.org/10.1111/nep.12054. PubMed.

5 Hardak E, Brook O, Yigla M. Radiological features of Pneumocystis jirovecii Pneumonia in immunocompromised patients with and without AIDS. Hai. 2010;188(2):159–63. doi: http://dx.doi.org/10.1007/s00408-009-9214-y. PubMed.

6 Boiselle PM, Crans CA, Jr, Kaplan MA. The changing face of Pneumocystis carinii pneumonia in AIDS patients. AJR Am J Roentgenol. 1999;172(5):1301–9. doi: http://dx.doi.org/10.2214/ajr.172.5.10227507. PubMed.

7 Ebner L, Walti LN, Rauch A, Furrer H, Cusini A, Meyer AM, et al. Clinical course, radiological manifestations, and outcome of Pneumocystis jirovecii pneumonia in HIV patients and renal transplant recipients. PLoS One. 2016;11(11):. doi: http://dx.doi.org/10.1371/journal.pone.0164320. PubMed.

8 Ledergerber B, von Overbeck J, Egger M, Lüthy R. The Swiss HIV Cohort Study: rationale, organization and selected baseline characteristics. Soz Praventivmed. 1994;39(6):387–94. doi: http://dx.doi.org/10.1007/BF01299670. PubMed.

9 Koller MT, van Delden C, Müller NJ, Baumann P, Lovis C, Marti HP, et al. Design and methodology of the Swiss Transplant Cohort Study (STCS): a comprehensive prospective nationwide long-term follow-up cohort. Eur J Epidemiol. 2013;28(4):347–55. doi: http://dx.doi.org/10.1007/s10654-012-9754-y. PubMed.

10 Hansell DM, Bankier AA, MacMahon H, McLoud TC, Müller NL, Remy J. Fleischner Society: glossary of terms for thoracic imaging. Radiology. 2008;246(3):697–722. doi: http://dx.doi.org/10.1148/radiol.2462070712. PubMed.

11 Tasaka S, Tokuda H, Sakai F, Fujii T, Tateda K, Johkoh T, et al. Comparison of clinical and radiological features of pneumocystis pneumonia between malignancy cases and acquired immunodeficiency syndrome cases: a multicenter study. Intern Med. 2010;49(4):273–81. doi: http://dx.doi.org/10.2169/internalmedicine.49.2871. PubMed.

12 Lichtenberger JP, 3rd, Sharma A, Zachary KC, Krishnam MS, Greene RE, Shepard JA, et al. What a differential a virus makes: a practical approach to thoracic imaging findings in the context of HIV infection--part 1, pulmonary findings. AJR Am J Roentgenol. 2012;198(6):1295–304. doi: http://dx.doi.org/10.2214/AJR.11.8003. PubMed.

13 Kanne JP, Yandow DR, Meyer CA. Pneumocystis jiroveci pneumonia: high-resolution CT findings in patients with and without HIV infection. AJR Am J Roentgenol. 2012;198(6):W555–61. doi: http://dx.doi.org/10.2214/AJR.11.7329. PubMed.

14 Kuhlman JE, Kavuru M, Fishman EK, Siegelman SS. Pneumocystis carinii pneumonia: spectrum of parenchymal CT findings. Radiology. 1990;175(3):711–4. doi: http://dx.doi.org/10.1148/radiology.175.3.2343118. PubMed.

15 Fujii T, Nakamura T, Iwamoto A. Pneumocystis pneumonia in patients with HIV infection: clinical manifestations, laboratory findings, and radiological features. J Infect Chemother. 2007;13(1):1–7. doi: http://dx.doi.org/10.1007/s10156-006-0484-5. PubMed.

Appendix 1

Classification of imaging patterns

Summary of recorded imaging patterns: 1 – ground glass opacity (GGO) (increase in lung attenuation without obscuring pulmonary vessels), 2 – mosaic ground glass opacity (alternating GGO adjacent to hypoattenuating lung with sharp demarcation), 3 – ground glass nodule (GGN, nodule with ground-glass density), 4 – mixed nodule (mixN, nodule with a solid center and peripheral halo of GGO with a minimal width of 1 mm), 5 – smooth, solid nodule (N, well-demarcated dense nodule), 6 – lobulated, solid nodule (IN, convex outpouchings), 7 – spiculated, solid nodule (sN, linear radiations extending from the nodule), 8 – cavitary nodule (cN, presence of gas in the nodule), 9 – oval nodule (oN), 10 – calcified nodule (Ca++N, nodule with a density greater than 200 HU), 11 – tree-in-bud (well-defined pulmonary nodules with centrilobular branching opacities), and 12 – centrilobular nodules (cluster of small, peribronchovascular nodules). Furthermore, interstitial lung densities were classified as follows: 13 – reticulation (fine reticular grid and thickened interlobular septa), 14 – linear opacities (linear densities of > 1 mm thickness), 15 – coarse reticulation (thick reticular grid), 16 – beaded septum sign (nodular thickening of interlobular septa), 17 – honeycombing (peripheral cysts within a coarse reticulation), 18 – bulla (round hypoattenuation >1 cm with no or thin wall), 18.1 – centrilobular emphysema (centrilobular areas of decreased attenuation, generally without visible walls), 18.2 – panacinar emphysema (decrease in lung parenchyma, several adjacent bullae, and no normal lung in between); 18.3 – paraseptal emphysema (subpleural string of bullae), and 19 – cyst (round hypoattenuation with a thin wall < 2 mm).

Air-space disease was classified as follows: 20 – air-space disease (AS, dense acinar consolidation) and 20.1 – air-space disease with positive bronchogram (consolidation with branching hyperlucencies). Pleural disease was divided into the following patterns: 21 – pleural thickening (pleura > 1 mm thick), 21.1 – pleural thickening with adjacent reticulation, 22 – nodular pleural thickening (< 10 mm), 22.1 – nodular pleural thickening (> 10 mm), 23 – pleural plaque (rectangular pleural thickening), 24 – pleural scar (pleural thickening > 10 mm), 25 – pleural effusion, and 25.1 – loculated effusion.

Finally, airway diseases were classified with the following patterns: 26 - bronchial cuffing (diffuse thickening of the bronchial wall), 27 – focal bronchial thickening (segmental thickening of the bronchial wall), 28 - bronchial secretion (hypoattenuating bronchial fluid), 29 – mucus plugging (dense content in segmental dilated bronchus), 30 – bronchiectasis (bronchus with a larger diameter than the accompanying artery), 31 – (sub-)segmental volume loss (small lung segments with a concentration of vessels), and 32 – segmental air trapping (hypoattenuating lobule with separated vessels). In addition, the radiologists recorded the presence of pleural effusions and hilar and mediastinal lymphadenopathies (node > 1 cm). Furthermore, the distribution of the parenchymal changes within the lung (segmental and central versus subpleural distribution) was noted [7].